

See discussions, stats, and author profiles for this publication at: <https://www.researchgate.net/publication/228326147>

Electronic Structure of FePc and Interface Properties on Ag(111) and Au(100)

ARTICLE in THE JOURNAL OF PHYSICAL CHEMISTRY C · MAY 2012

Impact Factor: 4.77 · DOI: 10.1021/Jp302233e

CITATIONS

31

READS

102

7 AUTHORS, INCLUDING:



Fotini Petraki

28 PUBLICATIONS 404 CITATIONS

SEE PROFILE



Heiko Peisert

University of Tuebingen

127 PUBLICATIONS 2,630 CITATIONS

SEE PROFILE



Umut Aygöl

University of Tuebingen

14 PUBLICATIONS 168 CITATIONS

SEE PROFILE



Thomas Chassé

University of Tuebingen

230 PUBLICATIONS 2,570 CITATIONS

SEE PROFILE

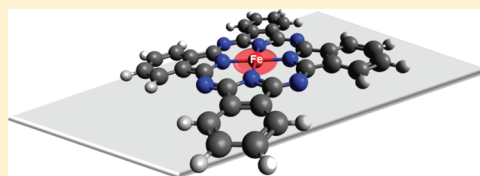
Electronic Structure of FePc and Interface Properties on Ag(111) and Au(100)

F. Petraki,[†] H. Peisert,^{*,†} U. Ayg  l,[†] F. Latteyer,[†] J. Uihlein,[†] A. Vollmer,[‡] and T. Chass  [†]

[†]IPTC, University of Tuebingen, Morgenstelle 18, 72076 Tuebingen, Germany

[‡]Helmholtz Centre Berlin for Materials and Energy, Electron storage ring BESSY II, Albert-Einstein-Str. 15, 12489 Berlin, Germany

ABSTRACT: The electronic structure of iron phthalocyanine (FePc) and interface properties on Ag(111) and Au(100) are investigated by photoexcited electron spectroscopies: photoemission (XPS and UPS) and X-ray absorption spectroscopy (XAS or NEXAFS). Valence band structures with Fe character were identified using resonant photoemission. The strength and nature of the interaction at the interface depend clearly on the substrate. A strong interaction of the central metal atom of the phthalocyanine occurs on Ag(111), whereas no significant changes of the electronic situation were found for FePc on Au(100). Resonant photoemission data show that for FePc on Ag(111) the formed interface states close to the Fermi level are determined by the interaction between Fe 3d states and substrate related states. On the other hand, also the nitrogen atom of FePc is involved in the interaction.



1. INTRODUCTION

The recently increasing research efforts devoted to transition metal phthalocyanines (TMPcs) derives from their unique optical, electronic, and magnetic properties. Metal phthalocyanines can be applied in a variety of devices. Most recently, optoelectronic devices such as light-emitting diodes, field-effect transistors, and solar cells are in the focus of research (e.g., refs 1 and 2). In addition, magnetic properties of the TMPcs are studied intensely, driven, e.g., by possible future applications in spintronic nanodevices such as spin valves.^{3–7} However, the electronic configuration and thus the magnetic properties of the central metal atom of the TMPc is not completely understood and has been intensively debated during the last years.^{8–17} Moreover, at interfaces, the electronic configuration may change, which is in particular important for spintronic devices, since the electron (spin) injection occurs at these interfaces.

Recent studies have shown that the strength and nature of the interaction between Pcs and metallic substrates (Au, Ag) depend clearly on the central metal atom of the Pc. In particular, for open shell molecules such as CoPc, charge transfer from the central metal atom of the Pc at the interface to the substrate occurs as a direct consequence of the adsorption of the molecule. This is concluded from change of both photoemission (XPS) and X-ray absorption (XAS) spectra directly at the interface.^{18,19} On the other hand, changes in XPS and XAS spectra are weaker for MnPc on Au and Ag, but nevertheless charge transfer processes at the interface are likely.^{20,21} In order to predict more general inside in the interaction of TMPs to Au and Ag, we focus in the present work on iron phthalocyanine (FePc), where the electronic configuration of the central metal ion Fe²⁺ is d⁶, i.e., between Co²⁺ and Mn²⁺.

2. EXPERIMENTAL SECTION

The measurements were performed at the third generation synchrotron radiation source BESSY II (Berlin) using the Optics-beamline and the endstation SURICAT. The photon energies were calibrated comparing the binding energy (BE) of Au 4f_{7/2} and Ag 3d_{5/2} peaks excited by first- and second-order light. The energy resolution for XPS and XAS was set to ≈ 100 meV at a photon energy of 400 eV. The absorption was monitored indirectly by measuring the total electron yield (TEY), i.e., sample current. The spectra were normalized to have the same absorption edge step height well above threshold. The energy resolution in the case of resonant photoemission (ResPES) was set to about 200 meV.

As substrates, we used Au(100) and Ag(111) single crystals, cleaned by argon ion sputtering and annealing. The cleanliness was checked by X-ray photoemission spectroscopy (XPS). FePc powder was carefully cleaned by vacuum sublimation prior use. Thin films of FePc were evaporated in ultrahigh vacuum (base pressure $< 1 \times 10^{-8}$ mbar) from a temperature-controlled cell with evaporation rates between 0.1 and 0.5 nm/min. The nominal film thickness was estimated from both a quartz microbalance and from XPS intensity ratios using element and energy dependent sensitivity factors from ref 22 and assuming layer-like growth.

3. RESULTS AND DISCUSSION

I. Bulk Electronic Structure. Polarization dependent X-ray absorption spectroscopy (XAS), also called near edge X-ray absorption fine structure (NEXAFS) spectroscopy, probes the absorption of the X-rays due to excitations from a core level into lower unoccupied states as a function of energy. The

Received: March 7, 2012

Revised: April 27, 2012

Published: April 30, 2012

method provides information about the molecular orientation as well as about the electronic structure of the material under consideration.

First, we will discuss the orientation of the organic molecules on the studied substrates. Although in general the molecular orientation of phthalocyanine molecules can be extracted from both N 1s and C 1s excitation spectra, a common carbon contamination of beamline components often hinders the detailed analysis of carbon edges; thus, we consider polarization dependent N K edge spectra. In Figure 1, a series of XAS

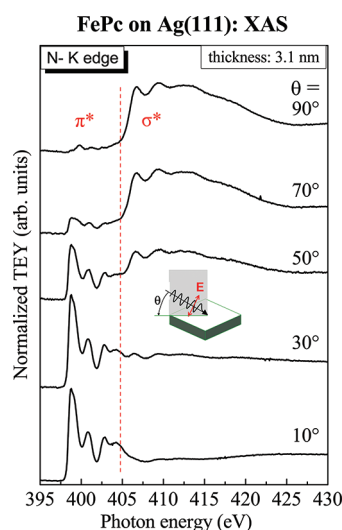


Figure 1. N 1s excitation spectra of an about 3 nm thick FePc film on Ag(111). The lower energy features ($E < 405$ eV) represent the π^* resonances, whereas those features above 405 eV are related to the σ^* resonances. The sketch illustrates the experimental geometry for p-polarized light. The angular dependence indicates flat-lying molecules with a high degree of orientation.

spectra as a function of the angle θ between the surface normal and the electric field vector of the p-polarized synchrotron light (see inset of Figure 1) is shown for a 3.1 nm thick FePc film on Ag(111). Following the interpretation of N K-edge XAS spectra of related Pcs (see, e.g., ref 23), at grazing beam incidence, a maximum intensity of the dipolar transitions into groups of individual π^* states (photon energy 395–405 eV) is expected, when the molecules are lying flat on the sample surface. The opposite behavior is expected for the $1s \rightarrow \sigma^*$ resonances above photon energies of 405 eV.

From Figure 1, it can be seen that the relative intensities of the spectral features vary strongly with the angle θ of the incident radiation; the maximum intensity of the π^* transitions is found at grazing incidence ($\theta = 10^\circ$) and decreases with increasing angle of incidence, reaching a minimum at normal incidence ($\theta = 90^\circ$). The almost vanishing intensity at normal incidence indicates that the FePc molecules are well oriented on the metallic surface and lying with their molecular planes parallel to the substrate. The weak residual spectral intensity in the range of π^* resonances at $\theta = 90^\circ$ is not necessarily caused by an imperfect ordering, it might be associated with weak, in plane polarized transitions in the same energy range as the π^* resonances.^{23–25} A possible reason is a hybridization of unoccupied nitrogen-related states with the d-orbitals of the transition metal atom which depend on the central metal atom of the Pc as recently discussed for related systems.^{15,16}

Valuable information about the electronic structure of the central metal atom in TMPcs can be acquired from the polarization dependent 2p excitation spectra (i.e., Fe $L_{2,3}$ XAS spectra), in particular, if the molecules are highly ordered and the molecular orientation is known. In Figure 2, the related Fe

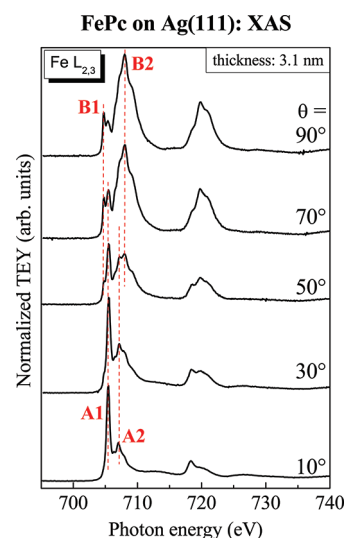


Figure 2. Fe 2p excitation spectra of an about 3 nm thick FePc film on Ag(111). A clear angular dependence is also visible for the Fe 2p resonances.

2p excitation spectra are depicted for a FePc coverage of about 3.1 nm on Ag(111). The general spectral features are in good agreement with recently reported data for the FePc/Au(110) interface,^{15,16} but the angular dependence seems to be more pronounced compared to the data of ref 16. At the chosen film thickness, mainly bulk properties of the phthalocyanine molecule are mapped. The features in the photon energy region between 702 and 712 eV are due to transitions from the Fe $2p_{3/2}$ orbitals into unoccupied d orbitals (L_3 spectra), while the broad feature in the range 717–725 eV is attributed to transitions from the Fe $2p_{1/2}$ levels (L_2 spectra). Due to the known absorption geometry of the molecules, from angle dependent XAS, conclusions can be drawn related to the different empty molecular orbitals. Clearly visible from Figure 2 are two groups of Fe $2p_{3/2}$ excitations with different polarization dependence: At grazing incidence, the intensity at 705.5 and 707.15 eV (features A1 and A2) is maximal, whereas at normal incidence an additional peak at lower photon energy (B1 at 704.8 eV) and a group of excitations between 706 and 710 eV with the maximal intensity at 708.0 eV (denoted B2) dominate the spectrum. Related to the molecular axis, the A features are transitions polarized perpendicular to the molecular plane (z-polarized) and the B features are polarized within the molecular plane (xy-polarized). Interestingly, the B1 feature at low photon energies was not observed for CoPc thin films,²⁶ and besides transitions into $d_{x^2-y^2}$, this polarization dependence (increasing intensity with increasing θ) is only expected for d_{xy} . Since from crystal field splitting two holes can be expected in the $d_{x^2-y^2}$ orbital with the highest energy, the presence of B1 may point to a partially empty d_{xy} orbital, as suggested in ref 17. However, for the Fe 2p excitation spectra, the final state of the X-ray absorption process consists of a partly filled $2p^5$ core state and of incompletely filled 3d-valence states (d^7). The shape of the XAS spectra is therefore

FePc on Ag(111): Resonant Photoemission

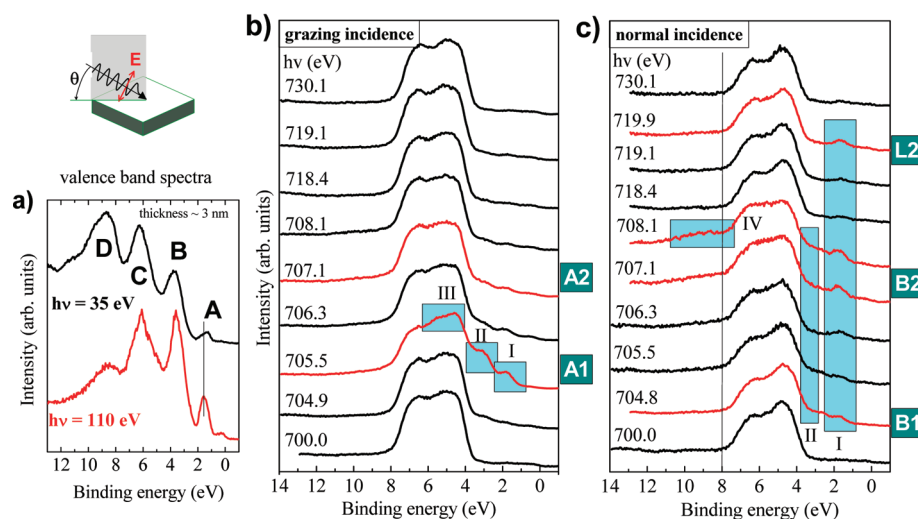


Figure 3. (a) Valence band spectra at photon energies where photoemission high cross sections for FePc related features are high. (b and c) Resonant photoemission spectra in the range of the Fe $2p_{3/2}$ absorption edge for FePc on Ag(111) at grazing incidence (b) and normal incidence (c). Although the main features are determined by the substrate, the intensity enhancement at the resonance energies indicates valence band features with Fe character.

determined to a large extent by multiplet effects, caused by the strong overlap of the core wave function with the valence wave functions (for a detailed discussion, see, e.g., ref 27), which makes a discussion of the ground state electronic configuration more complicated.

Resonant photoemission spectroscopy (ResPES) can be further utilized for the experimental analysis of the contribution of different chemical species to spectral valence band features (see, e.g., refs 26 and 28). In Figure 3a, valence band spectra for a 3.1 nm thick FePc film on Ag(111) are displayed, at photon energies where photoemission cross sections for FePc related features are high. At 35 eV, in particular, C 2p and N 2p cross sections are high, whereas, at 110 eV, the relative spectral weight of Fe 3d is increased.^{28,29} Both spectra in Figure 3a show four spectral features located at about 1.4 eV (A), 3.7 eV (B), 6.2 eV (C), and 8.7 eV (D). The increase of the relative intensity of the HOMO related peak at $h\nu = 110$ eV indicates a contribution of Fe 3d levels to this feature.

If an electron is resonantly excited into unoccupied molecular levels (i.e., at the photon energies of the XAS resonances), different possible nonradiative deexcitation channels of the resulting core hole cause substantial changes in spectral valence band features: normal Auger electron emission, participator decay (ResPES), and spectator decay (resonant Auger spectroscopy). In order to understand in particular the contribution of the central metal atom of FePc to valence band features, ResPES measurements at the Fe $L_{3,2}$ edge were performed; the spectra are displayed in Figure 3b and c. In the case of a participator decay process, the excitation into an empty state induces an enhancement of spectral features with contributions of the metal atom. Note that, due to the photoemission cross sections at these photon energies, the spectral features in Figure 3 essentially originate from the Ag substrate. However, enhancements of overlayer related features, denoted I–IV, are clearly visible upon tuning the excitation energy across the Fe L absorption edge in the range from 700 to 730.1 eV. Binding energies of peaks I and II are 1.8 and 3.3 eV, respectively. A broadened feature III is visible at about 5 eV.

At these energies, metal related states can be expected.²⁸ Further intensity enhancements are visible at higher binding energies (IV). The enhancement of different structures depends on the polarization of the incoming light. At grazing incidence (z -polarized related to the molecular axis or out of plane), the main effect is observed at the most prominent resonance A1 (cf. also Figure 2) and minor effects at A2; the intensity of features I–III increases distinctly at A1. The absence of a clear background increase suggests that the excited electron remains at the Fe atom within the time scale of the deexcitation process and thus the Fe-related states are localized analogously to CoPc.²⁶ On the other hand, the enhancement of *three* spectral features indicates that different electrons (with different binding energies) can be emitted after the excitation of an electron into the empty z -polarized level. This was not observed for CoPc and may point to a mixing of different electronic configurations, as suggested in ref 17. Looking further at the ResPES data at normal incidence (in plane, transitions, xy -polarized) in Figure 3c, again the HOMO related feature I is enhanced at both resonance energies B1 and B2, moreover at an energy within the L_2 -edge (denoted L2). This behavior might be a further hint for the presence of mixed valences. In addition, in the range of the B2 resonance, broad features above binding energies of 6 eV appear, denoted as IV in Figure 3c. The presence of such broad features at binding energies where no Fe-related features are expected²⁹ cannot be understood by participator decay processes; they might be induced either by spectator decay or by normal Auger processes. Since in the case of Auger transitions the excited electron does not remain at the Fe atom, the presence of feature IV at the resonance B2 may point to a more delocalized xy -polarized Fe related state compared to the z -polarized states, as recently observed for CoPc.²⁶

II. Interface Properties. III. The FePc/Ag(111) Interface.

As mentioned above, the electronic configuration may change at interfaces. In particular, for open shell TMPcs, charge transfer processes, involving the central metal atom of the Pc, were observed.^{18,19} In this context, photoemission and X-ray

absorption spectroscopies are valuable tools, since these methods probe directly the occupied and unoccupied electronic structure.

First, we discuss Fe 2p photoemission spectra in Figure 4. Here, we should keep in mind that a nominal monolayer

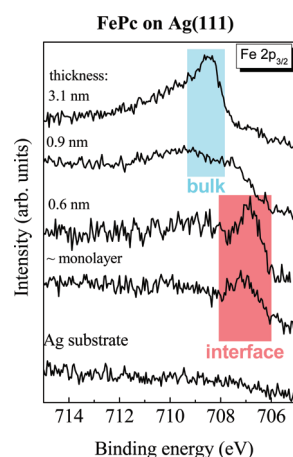


Figure 4. Evolution of the Fe 2p_{3/2} XP spectra during the FePc/Ag(111) interface formation. The colored frames illustrate the development of a new interface component.

corresponds to about 0.03 monolayer Fe atoms on the surface, only. The bulk spectrum (3.1 nm) is in good agreement with the literature.³⁰ The main line at 708.4 eV exhibits a broad asymmetry at the high binding energy side which can be ascribed to multiplet structures due to the coupling of the core hole to d-holes of the valence band (see above). Significant differences in the spectral shape are observed between the monolayer (ML) and the thick film. Whereas bulk specific features disappeared in the ML spectrum, a new peak is developed located at about 1.5 eV lower binding energy, close to the expected value for metallic Fe. In general, energetic shifts to lower binding energies at the interface to a metal can be understood by charge transfer processes or alternatively by a final state effect in photoemission. The latter can be related to charge transfer screening, as recently observed in Auger and/or photoemission lines of related systems.^{31–33} The series of Fe 2p spectra in Figure 4 remind however to the system CoPc/Ag, where analogously an additional Co 2p peak appears at the interface¹⁸ and charge transfer processes were evident by the application of a broad variety of methods.^{18,19,34} Moreover, the different shape of the ML spectrum compared to the thick film indicates that the multiplet splitting has changed and, thus, points to a different electronic configuration of the involved d-levels.

If the electronic structure of the molecules is changed at the interface, Fe 2p excitation spectra should be particularly affected. Fe L₃ XAS spectra as a function of the film thickness are shown in Figure 5; we chose the prominent angles grazing incidence (out of plane excitations, Figure 5a) and normal incidence (in plane excitations, Figure 5b). In both cases, distinct changes in the spectra are indeed visible going from the bulk (3.1 nm) to monolayer coverage. At grazing incidence, a new feature labeled as A0 is developed at the interface, which is hardly visible in the bulk spectrum (3.1 nm), whereas A1 and A2 disappear at the metal interface. In a first view, one might assume that the features are simply energetically shifted to higher photon energies due to the lowering of the Fe 2p

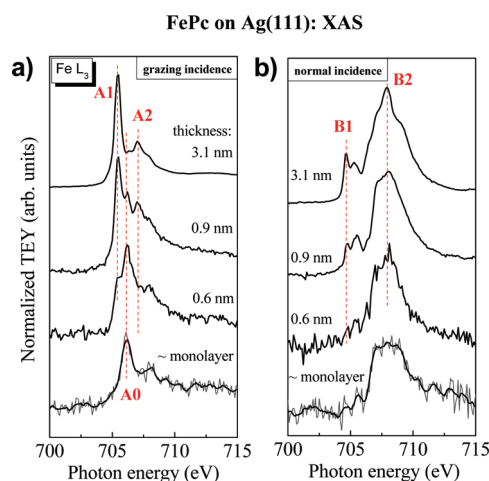


Figure 5. Fe L₃ absorption spectra acquired at grazing (a) and normal (b) incident light as a function of the FePc film thickness ranging from monolayer to 3.1 nm deposited on Ag(111) substrate.

binding energy at the interface (the initial level of the absorption process). However, the Fe 2p binding energy shift (1.5 eV) is much larger than the energetic distance between A1 and A0 (~0.7 eV). Also, the spectra for in plane transitions (Figure 5b) change drastically: the B1 feature disappears, and the shape of B2 is clearly different going from the thick film to the monolayer. In particular, the appearance of a feature A0 is also similar to the system CoPc/Ag(111). A possible origin of A0 is transitions into a new (unoccupied) electronic level formed due to an interaction between wave functions of the phthalocyanine's central metal atom and the substrate.²⁰ We conclude therefore that the interaction of FePc is very similar to that of CoPc on the Ag(111) substrate.

The question arises, if there is a hybridization between the d-levels of the central metal atom of the phthalocyanine and the neighbored nitrogen p-levels,^{14–16,35} whether or not the nitrogen atom is also involved in the interaction with the Ag(111) substrate. In Figure 6, we show N K excitation spectra for the N 1s → π^* transitions at grazing incidence as a function of the FePc coverage. At least two peaks contribute to the N 1s

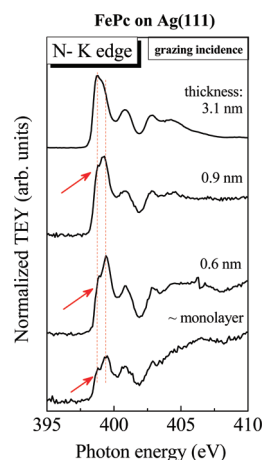


Figure 6. N K-edge absorption spectra acquired at grazing incidence of the incoming synchrotron light as a function of the FePc film thickness from monolayer to 3.1 nm deposited on Ag(111). The change of the shape of the π^* resonance points to an involvement of nitrogen in the interface interaction.

→ π^* resonance, where the leading peak is visible as a shoulder on the low photon energy side in Figure 6; the splitting can be understood by the hybridization between nitrogen and metal related states, as recently discussed for other TMPcs.^{20,35} It is clearly visible that the relative intensity of the shoulder changes with the film thickness (see arrow in Figure 6). The decrease of the relative intensity at low coverages may point to a partial filling of the corresponding level and therefore indicates involvement of nitrogen in the interaction at the interface.

An interaction at interfaces associated with a splitting of electronic states due to hybridization can be observed directly in the corresponding valence band photoemission spectra. A formation of such new states, expressed by a splitting of HOMO related features in the spectra, was recently observed for TMPcs on metal substrates, such as CoPc and FePc on Au.^{18,34} In Figure 7, we present valence band spectra for FePc

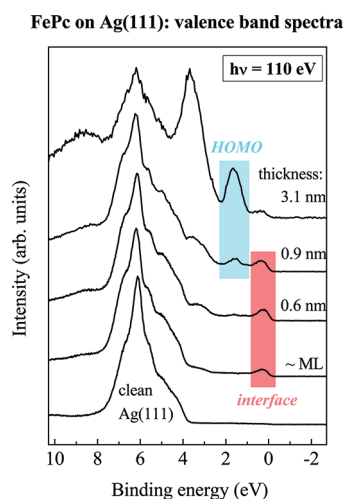


Figure 7. Valence band spectra for FePc on Ag(111) as a function of the film thickness taken at a photon energy of 110 eV. Formation of an interface state close to the energy of the Fermi level is clearly visible.

on Ag(111) as a function of the film thickness. It can be seen how spectral features of the phthalocyanine develop with increasing film thickness (compare also Figure 3a). The valence band spectra in the monolayer range however show clearly additional intensity in the energy range of the Fermi level, whereas the HOMO becomes first visible at coverages of more than 1 monolayer. The energy separation of both peaks is about 1.2 eV. We denote therefore the new state at the Fermi level as the interface state in Figure 7. The intensity of the interface and the HOMO peak is nearly the same at a film thickness of 0.9 nm. Assuming that only the first layer interacts with the Ag substrate and the absence of islands in the first steps of the deposition, this indicates a coverage of less than 2 monolayers; i.e., our nominal film thickness might be slightly overestimated.

We will study now if this interface state exhibits metal character. For this reason, ResPES measurements were performed for a monolayer coverage of FePc on Ag(111). The valence band spectra at excitation energies of Fe 2p resonances are presented in Figure 8 for grazing incidence (out of plane transitions) as well as for normal incidence (in plane transitions). In a first view, FePc related features in the bottom panels of Figure 8 are hardly visible on the background of the Ag derived features due to the photoemission cross section at these energies.²⁸ However, a zoom in the HOMO related region (top panels) reveals significant intensity enhancements

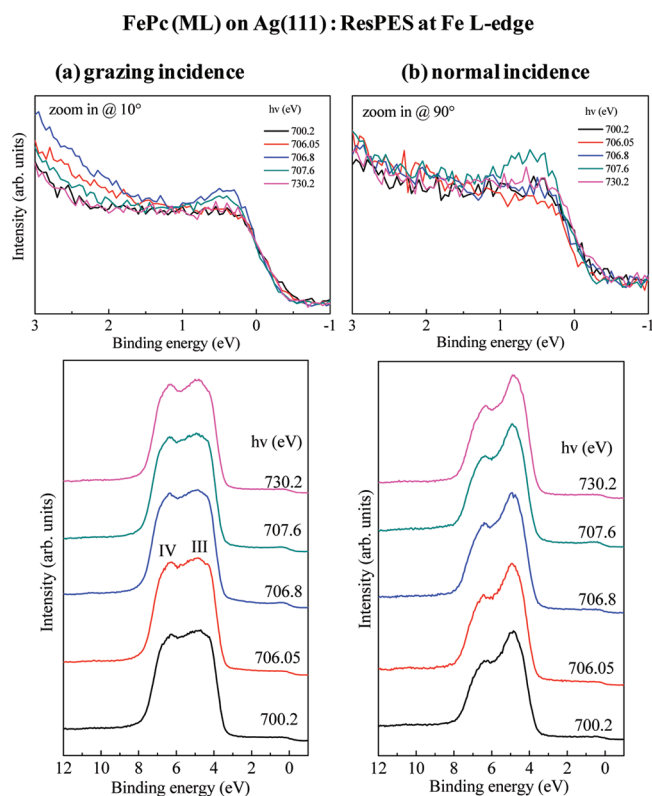


Figure 8. A series of valence band spectra recorded at excitation photon energy around Fe L-edge at grazing (a) and normal (b) incidence. In the upper part, we zoom in the low binding energy region, where a clear enhancement of the HOMO is displayed in both cases.

near the respective resonance energies. Although the same feature close to the Fermi level is enhanced for both in plane and out of plane transitions, the corresponding photon energies depend clearly on the polarization of the incoming light: For grazing incidence, the enhancement occurs at energies near A0 (~ 706.0 eV), whereas the strongest effects for normal incidence were observed near the B2 feature between 707 and 709 eV (cf. Figure 5). Other intensity variations are hardly visible in the spectra, but they might be overlapped by the intense Ag 4d band of the substrate. The data show that the formed interface states close to the Fermi level are determined by the interaction between Fe 3d states and substrate related states.

II.III. The FePc/Au(100) Interface. Although gold is believed to interact weakly with organic molecules such as phthalocyanines, charge transfer processes were observed in some cases, in particular for CoPc.^{18,19} In Figure 9, valence band spectra for FePc on Au(100) taken at a photon energy of 110 eV are shown for two prominent film thicknesses of 0.6 nm (a coverage of 1–2 monolayers) and 1.6 nm. In contrast to FePc on Ag (see above), no additional intensity close to the energy of the Fermi level is visible for low coverages, pointing to the absence of an interface state. Only an energetic shift of about 0.2 eV to higher binding energies is observed with increasing film thickness, which can be explained essentially by polarization screening, in detail discussed for ZnPc on Au(100) in ref 31.

The absence of an interface state for FePc on Au(100) can be further verified by XAS, where transitions into unoccupied states are probed. Fe 2p excitation spectra are displayed in Figure 10 as a function of the layer thickness. We note that

FePc on Au(100): valence band spectra

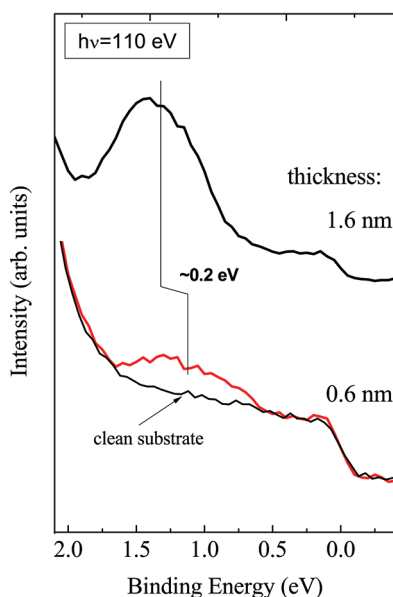


Figure 9. Valence band spectra for FePc on Au(100) taken at a photon energy of 110 eV. At a coverage of 1–2 monolayers (0.6 nm) in contrast to FePc on Ag, no additional intensity close to the energy of the Fermi level is visible, indicating the absence of an interface state.

FePc on Au(100)

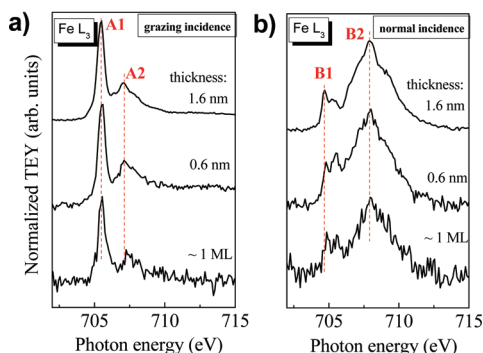


Figure 10. FePc on Au(100): Fe L_3 absorption spectra acquired at grazing (a) and normal (b) incident light as a function of the film thickness. No significant changes of the peak shape were observed, pointing to a weak interaction between the central metal atom of the phthalocyanine and the substrate.

analogously to FePc/Ag(111) angle dependent N K and Fe L absorption spectra (not shown) indicate that the molecules are well oriented parallel to the substrate surface. We focus in Figure 10 on the L_3 edge for the two prominent angles grazing incidence (a) and normal incidence (b); i.e., related to the molecular plane, we probe in plane and out of plane transitions. The absorption spectra for the thick FePc film on Au(100) are in good agreement with those recorded on Ag(111), revealing different groups of Fe $2p_{3/2}$ excitations with different polarization. However, contrary to FePc on Ag(111), no significant changes of the peak shapes are observed going from the thick film to the monolayer, even if the absence of small intensity variations cannot be ruled out completely due to the lower signal-to-noise ratio for lower coverages (e.g., of the B1 feature). In particular, a feature like A0—clearly observed for FePc on Ag(111) (cf. Figure 5a)—is not detectable at the FePc/Au(100) interface. This behavior reminds now to CoPc,

where an A0 interface feature was observed on Ag(111) but not on Au(100).²⁰

Even if the interaction between Fe of FePc and the Au(100) substrate is weak, the nitrogen atoms might interact with the substrate. N K-edge absorption spectra for two FePc film thicknesses on Au(100) are shown in Figure 11; we focus on

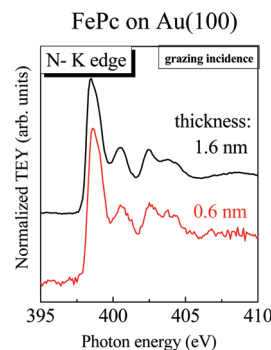


Figure 11. N K-edge absorption spectra acquired at grazing incidence of the incoming synchrotron light for two FePc film thicknesses on Au(100). In contrast to Ag(111), no change of the shape of the π^* resonance is visible.

the N $1s \rightarrow \pi^*$ transitions at grazing incidence of the incoming synchrotron light. In contrast to Ag(111) (Figure 6), no change of the shape of the π^* resonance is visible in comparison to the thicker film at a coverage of 0.6 nm (less than 2 monolayers), indicating the absence of a charge transfer to nitrogen in the case of the interface to Au(100). The charge transfer on Ag(111) may occur (i) directly between the substrate and nitrogen or (ii) via the central metal atom of the phthalocyanine due to the hybridization between nitrogen and Fe related states. Since for a related system, CuPc adsorbed on Ag(100), the N–Ag interaction gives rise to the strongest molecule–surface bonds,³⁶ a direct charge transfer cannot be ruled out. On the other hand, the dependence of the interaction between Pcs and metallic substrates on the central metal atom of the Pc and the metal character of the interface state for FePc on Ag(111) (see above) indicates that the interaction between the Fe atom of FePc and the substrate is crucial for the description of the interface.

The formation of interface states can be described by the interaction of wave functions between Fe of the molecule and the metal substrate, resulting in a pair of new levels. In this picture, the feature A0 for FePc on Ag(111) could be due to transitions into the new (unoccupied) electronic level. The energetic position of A0 depends on both the molecule and the substrate under consideration; therefore, for some systems, this feature may not be resolved in the spectra. However, in the case of FePc on Au(100), we do not have a further hint from photoemission for the formation of a new state at the interface; neither the valence band spectra (above) nor the Fe 2p photoemission spectra (not shown) exhibit additional features at low coverages. The absence of a strong interaction between the central metal atom of FePc and Au(100) agrees well with the recently studied system FePc/Au(111)¹⁷ but was not found for FePc/Au(110).^{15,34} Therefore, one may conclude that the orientation and the surface reconstruction of the substrate affects distinctly the properties of the interface under consideration.

4. SUMMARY

The electronic structure of FePc and interface properties on two substrates, Ag(111) and Au(100), were investigated. Valence band features with Fe derived character were identified using resonant photoemission; in particular, the appearance of a strong resonant participator deexcitation channel for out of plane transitions reveals a strong localization of these Fe related states.

The strength and nature of the interaction at the interfaces depends clearly on the particular noble metal substrate. For FePc on Ag(111), the experimental data reveal that the 3d-open shell is involved in an interfacial interaction through charge transfer with the substrate. On the other hand, no significant changes of the electronic situation were found for FePc on Au(100). The different electronic structure on both substrates may now have consequences for several applications in (opto-) electronic devices; e.g., the choice of electrode materials offers a route for a systematic tuning of the chemical interaction at the interface. As an example, hybrid interface states can tailor the spin injection properties in future hybrid spintronic devices combining organic semiconductors and (ferromagnetic) metal substrates as most recently demonstrated also for TMPcs.³⁷ The spin polarization at the inorganic/organic interface can be modified not only by the exchange of the transition metal of the phthalocyanine but also by surface properties as well as the choice of the substrate.

AUTHOR INFORMATION

Corresponding Author

*E-mail: heiko.peisert@uni-tuebingen.de. Phone: ++49 7071 29 76931.

Notes

The authors declare no competing financial interest.

ACKNOWLEDGMENTS

The work was supported by the German Research Council Ch 132/20-2. We acknowledge the Helmholtz-Zentrum Berlin - Electron storage ring BESSY II for provision of synchrotron radiation at the Optics-beamline. Financial travel support by BESSY is gratefully acknowledged. We thank W. Neu for technical support.

REFERENCES

- Pfeiffer, M.; Leo, K.; Zhou, X.; Huang, J. S.; Hofmann, M.; Werner, A.; Blochwitz-Nimoth, J. *Org. Electron.* **2003**, *4*, 89–103.
- Martinez-Diaz, M. V.; de la Torre, G.; Torres, T. *Chem. Commun.* **2010**, 46, 7090–7108.
- Domingo, N.; Bellido, E.; Ruiz-Molina, D. *Chem. Soc. Rev.* **2012**, *41*, 258–302.
- Annese, E.; Fujii, J.; Vobornik, I.; Panaccione, G.; Rossi, G. *Phys. Rev. B* **2011**, *84*, 174443.
- Cinchetti, M.; Heimer, K.; Wüstenberg, J.-P.; Andreyev, O.; Bauer, M.; Lach, S.; Ziegler, C.; Gao, Y. L.; Aeschlimann, M. *Nat. Mater.* **2009**, *8*, 115–119.
- Liu, Y. H.; Lee, T.; Katz, H. E.; Reich, D. H. *J. Appl. Phys.* **2009**, *105*, 07C708.
- Schmitt, F.; Sauther, J.; Lach, S.; Ziegler, C. *Anal. Bioanal. Chem.* **2011**, *400*, 665–671.
- Liao, M. -S.; Scheiner, S. *J. Chem. Phys.* **2001**, *114*, 9780–9791.
- Marom, N.; Kronik, L. *Appl. Phys. A: Mater. Sci. Process.* **2009**, *95*, 165–172.
- Maslyuk, V. V.; Aristov, V. Y.; Molodtsova, O. V.; Vyalikh, D. V.; Zhilin, V. M.; Ossipyan, Y. A.; Bredow, T.; Mertig, I.; Knupfer, M. *Appl. Phys. A: Mater. Sci. Process* **2009**, *94*, 485–489.
- Kroll, T.; Aristov, V. Yu.; Molodtsova, O. V.; Ossipyan, Yu. A.; Vyalikh, D. V.; Buechner, B.; Knupfer, M. *J. Phys. Chem. A* **2009**, *113*, 8917–8922.
- Piper, L. F. J.; Cho, S. W.; Zhang, Y.; DeMasi, A.; Smith, K. E.; Matsuura, A. Y.; McGuinness, C. *Phys. Rev. B* **2010**, *81*, 045201.
- Casarin, M.; Di Marino, M.; Forrer, D.; Sambì, M.; Sedona, F.; Tondello, E.; Vittadini, A.; Barone, V.; Pavone, M. *J. Phys. Chem. C* **2010**, *114*, 2144–2153.
- Kuz'min, M. D.; Hayn, R.; Oison, V. *Phys. Rev. B* **2009**, *79*, 024413.
- Betti, M. G.; Gargiani, P.; Frisenda, R.; Biagi, R.; Cossaro, A.; Verdini, A.; Floreano, L.; Mariani, C. *J. Phys. Chem. C* **2010**, *114*, 21638–21644.
- Bartolomé, J.; Bartolomé, F.; García, L. M.; Filoti, G.; Gredig, T.; Colesniuc, C. N.; Schuller, I. K.; Cezar, J. C. *Phys. Rev. B* **2010**, *81*, 195405.
- Stepanow, S.; Miedema, P. S.; Mugarza, A.; Ceballos, G.; Moras, P.; Cezar, C.; Carbone, C.; de Groot, F. M. F.; Gambardella, P. *Phys. Rev. B* **2011**, *83*, 220401(R).
- Petraki, F.; Peisert, H.; Biswas, I.; Chassé, T. *J. Phys. Chem. C* **2010**, *114*, 17638–17643.
- Petraki, F.; Peisert, H.; Biswas, I.; Aygüel, U.; Latteyer, F.; Vollmer, A.; Chassé, T. *J. Phys. Chem. Lett.* **2010**, *1*, 3380–3384.
- Petraki, F.; Peisert, H.; Latteyer, F.; Aygüel, U.; Vollmer, A.; Chassé, T. *J. Phys. Chem. C* **2011**, *115*, 21334–21340.
- Petraki, F.; Peisert, H.; Hoffmann, P.; Uihlein, J.; Knupfer, M.; Chassé, T. *J. Phys. Chem. C* **2012**, *116*, 5121–5121.
- Yeh, J. J.; Lindau, I. *At. Data Nucl. Data Tables* **1985**, *32*, 1–55.
- Peisert, H.; Biswas, I.; Knupfer, M.; Chassé, T. *Phys. Status Solidi B* **2009**, *246*, 1529–1545.
- Rocco, M. L. M.; Frank, K. -H.; Yannoulis, P.; Koch, E.-E. *J. Chem. Phys.* **1990**, *93*, 6859–6864.
- Floreano, L.; Cossaro, A.; Gotter, R.; Verdini, A.; Bavdek, G.; Evangelista, F.; Ruocco, A.; Morgante, A.; Cvetko, D. *J. Phys. Chem. C* **2008**, *112*, 10794–10802.
- Peisert, H.; Biswas, I.; Aygüel, U.; Vollmer, A.; Chassé, T. *Chem. Phys. Lett.* **2010**, *493*, 126–129.
- de Groot, F. M. F. *Coord. Chem. Rev.* **2005**, *249*, 31–63.
- Brühwiler, P. A.; Karis, O.; Mårtensson, N. *Rev. Mod. Phys.* **2002**, *74*, 703.
- Brena, B.; Puglia, C.; de Simone, M.; Coreno, M.; Tarafder, K.; Feyer, V.; Banerjee, R.; Gothelid, E.; Sanyal, B.; Oppeneer, P. M.; et al. *J. Chem. Phys.* **2011**, *134*, 074312.
- Ahlund, J.; Nilson, K.; Schiessling, J.; Kjeldgaard, L.; Berner, S.; Mårtensson, N.; Puglia, C.; Brena, B.; Nyberg, M.; Luo, Y. *J. Chem. Phys.* **2006**, *125*, 034709.
- Peisert, H.; Kolacyak, D.; Chassé, T. *J. Phys. Chem. C* **2009**, *113*, 19244–19250.
- Lukaszczuk, T.; Flechtner, K.; Merte, L. R.; Jux, N.; Maier, F.; Gottfried, J. M.; Steinrück, H.-P. *J. Phys. Chem. C* **2007**, *111*, 3090–3098.
- Schöll, A.; Zou, Y.; Schmidt, T.; Fink, R.; Umbach, E. *J. Phys. Chem. B* **2004**, *108*, 14741–14748.
- Gargiani, P.; Angelucci, M.; Mariani, C.; Betti, M. G. *Phys. Rev. B* **2010**, *81*, 085412-1–085412-7.
- Javaid, S.; Bowen, M.; Boukari, S.; Joly, L.; Beaufrand, J. -B.; Chen, Xi; Dappe, Y. J.; Scheurer, F.; Kappler, J. -P.; Arabski, J.; et al. *Phys. Rev. Lett.* **2010**, *105*, 077201-1–077201-4.
- Mugarza, A.; Lorente, N.; Ordejón, P.; Krull, C.; Stepanow, S.; Bocquet, M.-L.; Fraxedas, J.; Ceballos, G.; Gambardella, P. *Phys. Rev. Lett.* **2010**, *105*, 115702.
- Lach, S.; Altenhof, A.; Tarafder, K.; Schmitt, F.; Ehesan Ali, Md.; Vogel, M.; Sauther, J.; Oppeneer, P. M.; Ziegler, C. *Adv. Funct. Mater.* **2012**, *22*, 989–997.